Electrochemical Impedance Spectroscopy of Alloys in a Simulated Space Shuttle Launch Environment

L.M Calle[a,*], M.R. Kolody[b], R.D. Vinje[b], M.C. Whitten[c], and W. Li[d]

[a] *NASA, YA-C2-T, Kennedy Space Center, FL 32899*
[b] *ASRC Aerospace Corp., ASRC-20, Kennedy Space Center, FL 32899*
[c] *University of Central Florida, Orlando, FL 32826*
[d] *National Academies at NASA, YA-C2-T, Kennedy Space Center, FL 32899*

Abstract

Corrosion studies began at NASA/Kennedy Space Center in 1966 during the Gemini/Apollo Programs with the evaluation of long-term protective coatings for the atmospheric protection of carbon steel. An outdoor exposure facility on the beach near the launch pad was established for this purpose at that time. The site has provided over 35 years of technical information on the evaluation of the long-term corrosion performance of many materials and coatings as well as on maintenance procedures. Results from these evaluations have helped NASA find new materials and processes that increase the safety and reliability of our flight hardware, launch structures, and ground support equipment. The launch environment at the Kennedy Space Center (KSC) is extremely corrosive due to the combination of ocean salt spray, heat, humidity, and sunlight. With the introduction of the Space Shuttle in 1981, the already highly corrosive conditions at the launch pad were rendered even more severe by the acidic exhaust from the solid rocker boosters.

Over the years, many materials have been evaluated for their corrosion performance under conditions similar to those found at the launch pads. These studies have typically included atmospheric exposure and evaluation with conventional electrochemical methods such as open circuit potential (OCP) measurements, polarization techniques, and electrochemical impedance spectroscopy (EIS).

The atmosphere at the Space Shuttle launch site is aggressive to most metals and causes severe pitting in many of the common stainless steel alloys such as type 304L stainless steel (304L SS). A study was undertaken to find a more corrosion resistant material to replace the existing 304L SS tubing. This paper presents the results from atmospheric exposure as well as electrochemical measurements on the corrosion resistance of AL-6XN (UNS N08367) and 254-SMO (UNS S32154). Type 304L SS (UNS S30403) was used as a control. Conditions at the Space Shuttle launch pad were simulated by using a hydrochloric acid (HCl) and alumina (Al_2O_3) slurry rinse for the atmospheric exposure and an electrolyte consisting of 3.55% sodium chloride (NaCl) with increased concentrations of hydrochloric acid (HCl) for the electrochemical measurements. The results from both types of measurements revealed the superior corrosion performance of the higher-alloyed materials. Unlike 304L SS, 254-SMO and AL-6XN exhibited a significantly improved resistance to corrosion as the concentration of hydrochloric acid in the 3.55% NaCl electrolyte solution was increased.

Keywords: 304L, AL-6XN, 254-SMO, Electrochemical Measurements, EIS.

* Corresponding author, Fax: 01-321-867-4446
Email address: Luz.M.Calle@nasa.gov

1. Introduction

Type 304L Stainless Steel (304L SS) tubing is used in various supply lines that service the Orbiter at the Kennedy Space Center (KSC) launch pads. The acidic chloride environment, due to the ocean atmosphere and the fuel reaction in the solid rocket boosters, is aggressive to most metals and causes severe pitting in many of the common stainless steel alloys. 304L SS tubing is susceptible to pitting corrosion that can cause cracking and rupture of both high-pressure gas and fluid systems. The use of a new tubing alloy for launch pad applications would greatly reduce the possibility of failure, improve safety, lessen maintenance costs, and reduce downtime losses.

A previous investigation was undertaken in order to find a suitable replacement for 304L SS in vacuum jacketed cryogenic supply lines at the Space Shuttle launch sites. Of the nineteen alloys that were included in the investigation, several nickel-based alloys were found to have a very high resistance to corrosion in the highly corrosive environment at the launch pads [1-4].

In the present investigation, Electrochemical Impedance Spectroscopy (EIS) was used to study the corrosion performance of 254-SMO, AL-6XN, and 304L SS. Alloy 304L SS was included as a control. The EIS measurements were carried out under three different electrolyte conditions: neutral 3.55% NaCl, 3.55% NaCl in 0.1N HCl, and 3.55% NaCl in 1.0N HCl, which are referred to as Neutral, 0.1N, and 1N respectively throughout the paper. These conditions were expected to be less severe, similar, and more severe respectively than the conditions at the launch pad. In order to better understand the electrochemical results, surface analysis of the samples using Scanning Electron Microscopy (SEM), X-Ray Photoelectron Spectroscopy (XPS), and Auger Electron Spectroscopy (AES) was performed. Due to manuscript length limitations, most of the surface analysis results are not presented in this paper. A parallel study was carried out in which tubes fabricated with the alloys were exposed to the atmosphere at the KSC corrosion test site near the launch pads [5].

2. Experimental Procedures

2.1. Materials

Table 1 shows the actual chemical composition of the alloys in weight percentage. The test specimens were polished to 600-grit, ultrasonically degreased in a detergent solution and dried before immersion in the electrolyte.

Table 1: Chemical composition of stainless steel alloys (weight %)

Alloy	Fe	Ni	Cr	Mo	Mn	C	N	Si	P	S	Cu
304L	71.567	8.200	18.33	0.500	1.470	0.023	0.030	0.380	0.030	0.0002	0.460
AL-6XN	48.11	23.88	20.470	6.260	0.300	0.020	0.330	0.40	0.021	0.0003	0.200
254-SMO	55.162	17.900	20.000	6.050	0.490	0.012	0.196	0.350	0.019	0.001	0.680

2.2. EIS Measurements

A Model 378 Electrochemical Impedance system manufactured by EG&G Princeton Applied Research Corporation was used for all EIS measurements. The system includes: (1) the Model 273 Potentiostat/Galvanostat, (2) the Model 5210 Lock-In Amplifier, and (3) the Power Sine® Electrochemical Impedance Software. Data were gathered in the frequency range of 100 kHz to 0.01 Hz, with 10 mV AC amplitude.

The electrochemical cell included a saturated calomel reference electrode, a platinum-on-niobium counter electrode, the metal specimen working electrode, and a bubbler/vent tube. The tested alloy surface area was 1 cm^2.

Three different aerated electrolyte solutions were used, as indicated earlier: Neutral, 0.1N, and 1N. The solutions were aerated continuously for the duration of the EIS

measurements. Prior to the collection of EIS measurements, the open circuit potential (OCP) was monitored until the sample reached a potential that was stable within ±5 mV for a period of 10 minutes. The reported results are the averages of two or more runs.

An atmospheric exposure site near the launch pads was used to evaluate the corrosion performance of the alloys. Triplicate tubing samples of each alloy were exposed. An acid slurry was prepared by mixing 500 ml of a 10 percent (v/v) solution of HCl and 28.5 grams of alumina powder to simulate solid rocket booster deposition. One set of tubes was sprayed every two weeks with the acid slurry to accelerate the corrosion effect. The other set was left exposed to the natural marine seacoast environment.

2.3. Surface Morphology and Chemical Analysis

Morphology of the selected samples was observed by scanning electron microscopy (SEM) using a JEOL 5900LV scanning electron microscope. AES studies were conducted using a Physical Electronics 600 AES and XPS studies using a PHI 5400 spectrometer.

3. Results

3.1. Open Circuit Potential

Figure 1 shows the variation of OCP with immersion time for the alloys in the three different electrolytes. Figure 1 shows OCP versus time for 304L, 254-SMO, and AL-6XN in (a) Neutral, (b) 0.1N, and (c) 1N conditions. Data were collected for a period of 408 hours except for 304L SS under the 1N condition for which data collection was terminated when a color change in the electrolyte was observed, indicative of the loss of integrity of the sample.

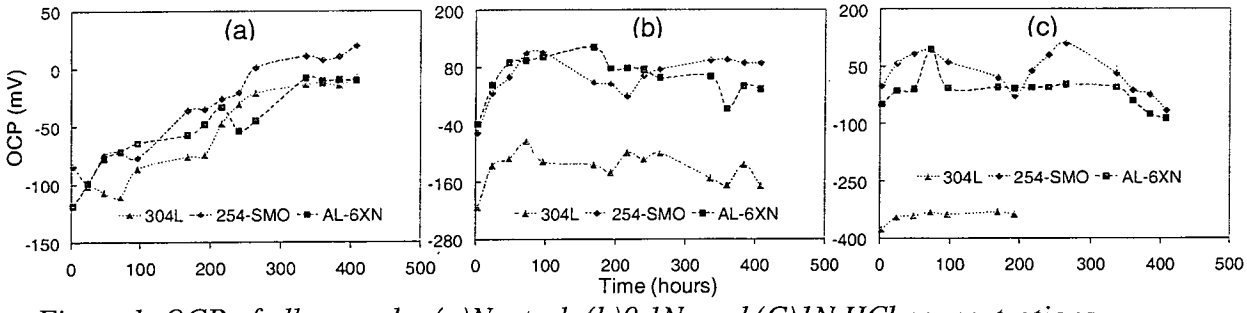

Figure 1. OCP of alloys under (a)Neutral, (b)0.1N, and (C)1N HCl concentrations.

3.2. Electrochemical Impedance Spectroscopy

Impedance data for the alloys in the three different electrolyte solutions were gathered. Representative Nyquist plots from one sample of each alloy in the three different electrolyte solutions are shown in Figure 2.

The majority of the Nyquist plots exhibited only one capacitive contribution represented by a semicircle. An equivalent circuit consisting of a parallel RC arrangement in series with the solution resistance, R_s, was used to simulate the data. In the simulation, a constant phase element (CPE), was used instead of the capacitance, C. The impedance of the equivalent circuit is given by [6,7]:

$$Z = R_s + \frac{R_p}{1 + (j\omega C R_p)^n}$$

where R_p is the passive film resistance or polarization resistance, C is the passive film capacitance, and n is a variable exponent used in fitting the data.

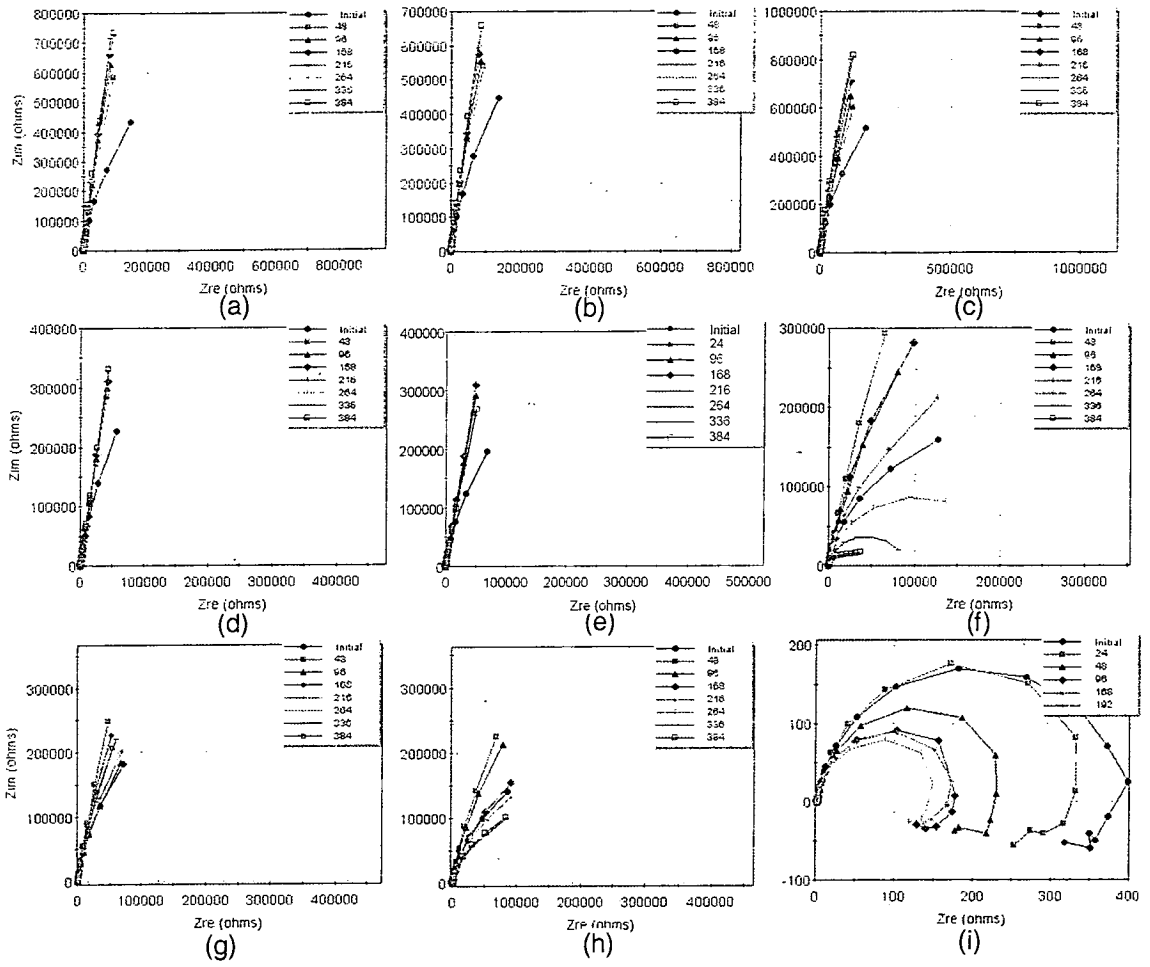

Figure 2. Nyquist plots of tested alloys at different immersion times (hrs): (a) 254-SMO, (b) AL-6XN, and (c) 304L in Neutral conditions; (d) 254-SMO, (e) AL-6XN, and (f) 304L in 0.1N conditions; (g) 254-SMO, (h) AL-6XN, and (i) 304L in 1N conditions.

Figure 3 shows the variation of R_p with immersion time for the three alloys in the three electrolyte solutions. Data collection for the 304L SS samples was terminated when a color change in the electrolyte solution was observed and the data became very noisy.

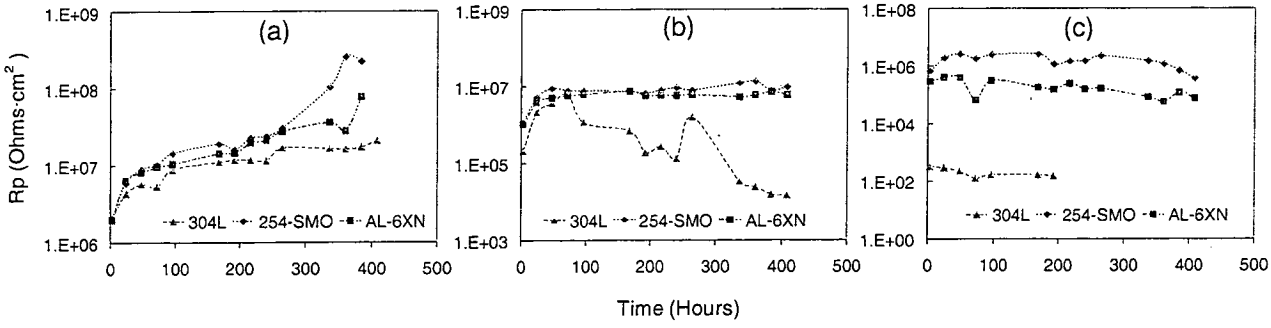

Figure 3. Average R_p at different immersion times: in (a)Neutral, (b)0.1N, and (c)1N conditions

Table 2 shows the average value for the final passive film resistance measured for all three alloys in different conditions.

Table 2. Final passive film resistance, R_p, measured for all three alloys in 3.55% NaCl with different HCl concentrations

Alloy	R_p, Neutral (Ohm · cm^2)	R_p, 0.1N (Ohm · cm^2)	R_p, 1.0N (Ohm · cm^2)
304L SS	2.12×10^7	1.49×10^4	1.58×10^2
254-SMO	2.24×10^8	9.44×10^6	3.79×10^5
AL-6XN	7.77×10^7	6.10×10^6	7.66×10^4

The thickness of the passive film is inversely related to the magnitude of the passive layer capacitance [8]. In this study, a CPE was used in the equivalent circuit instead of a pure capacitor. The deviation from a capacitor has been attributed to surface inhomogeneitites, roughness effects, and variations in properties or composition of surface layers [8]. The values obtained for the exponent in the CPE were between 0.98 and 0.86 (with the majority around 0.92). Since the exponent is close to one, CPE refers to the passive film capacitance, C. Figure 4 shows the variation with immersion time of the inverse capacitance, for the three alloys in Neutral, 0.1N, and 1N solutions. Table 3 shows the average final values for *1/C* for the three alloys in different acidic conditions.

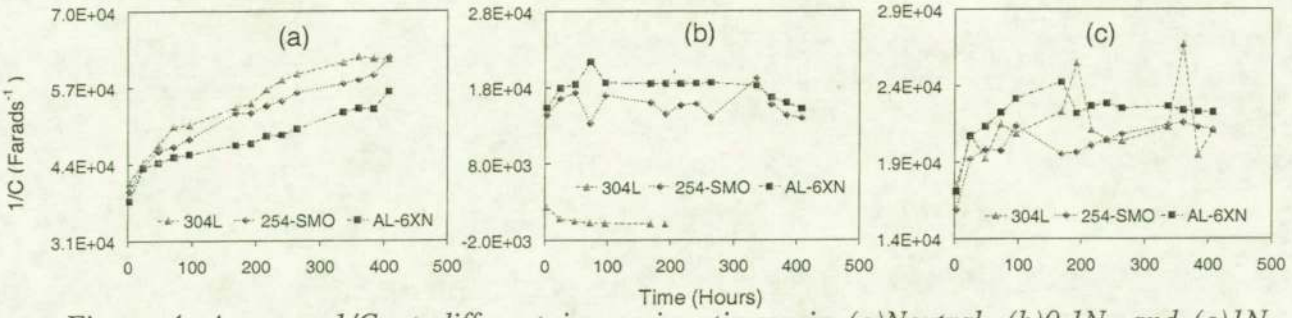

Figure 4. Average 1/C at different immersion times: in (a)Neutral, (b)0.1N, and (c)1N conditions

Table 3. Final 1/C measured values for all three alloys in different acid concentrations

Alloy	*1/C* in Neutral (Farads^{-1})	*1/C* in 0.1N (Farads^{-1})	*1/C* in 1N (Farads^{-1})
304L SS	6.18×10^4	2.11×10^4	1.63×10^2
254-SMO	6.22×10^4	2.11×10^4	1.40×10^4
AL-6XN	5.64×10^4	2.23×10^4	1.52×10^4

3.3. Surface Morphology

After the EIS analysis was complete, the 304L samples showed general corrosion under 1N test conditions, pitting and/or crevice corrosion in the 0.1N condition, and no sign of corrosion for the Neutral condition. Visually, the 254-SMO and AL-6XN samples did not show signs of corrosion. SEM images of 304L SS tested under 1N conditions are shown in Figure 5. The 304L-1N sample underwent general corrosion as seen in Figure 5(b).

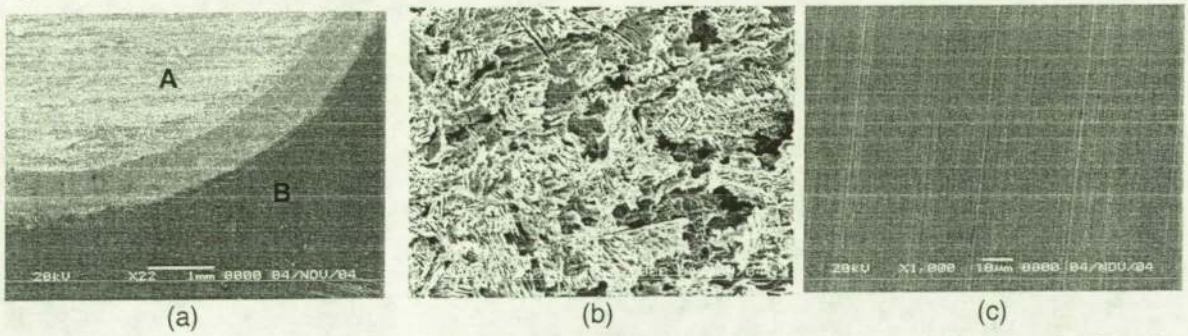

Figure 5. SEM images of 304L SS in 1N solution: (a) 22X imaging of the sample showing the exposed area A and unexposed area B, (b) 1000X image of A, and (c) 1000X image of B.

3.4. Atmospheric Exposure

The most important criterion of any laboratory test for corrosion is that it must consistently rank alloys according to their long-term service performance. The laboratory results were compared to those from a two-year atmospheric exposure study under conditions designed to simulate those present at KSC's Space Shuttle Launch Pads. Detailed results of the atmospheric exposure study have been reported elsewhere [5]. After two years of atmospheric exposure, 304L tubes were in poor condition with pits and brown spots over the entire surface, Al-6XN tubes were in good condition with only slight discoloration (light brown), and 254-SMO tubes were also in good condition. However, pitting spots were observed along a seam weld. The electrochemical results obtained in the present study agreed well with the atmospheric exposure. The EIS results indicated that one year of natural marine atmospheric exposure is more aggressive than 408 hours of immersion in the neutral 3.55% NaCl electrolyte solution.

4. Discussion

The open circuit potential gives an indication of how noble a metal is in a given environment and sometimes can be used to rank a material's resistance to corrosion. In general, a more positive OCP means higher corrosion resistance under the test conditions. Analysis of EIS results using an equivalent circuit model gives values for passive film resistance, R_p, and capacitance C. The passive film resistance is a direct measure of the corrosion resistance under open circuit conditions since the rate of corrosion is inversely proportional to the polarization resistance [6]. The inverse capacitance is proportional to the thickness of the passive film [8].

4.1. Alloys in Neutral 3.55% NaCl Conditions (Neutral)

The OCP for all three alloys in the Neutral solution steadily increased (Figure 1(a)) indicating that the alloys become more noble upon exposure to the salt solution. Figures 2(a)-(c) show an increase in corrosion resistance, as indicated by the increase of the diameter of the extrapolated semicircle. Accordingly, the calculated passive film resistance, R_p, increased for all three alloys (Figure 3(a)). This correlates well with the results obtained for the OCPs. A comparison at the end of the study showed that 254-SMO had the highest corrosion resistance, R_p, while 304L had the lowest. Normally, the initial corrosion rate of a metal is limited by the diffusion of corrosive components through the passive film. With time, a steady state is achieved when the rate of film growth equals the rate of dissolution into the aqueous phase [9]. For all three alloys, $1/C$ increased with immersion time (Figure 4(a)) indicating that the thickness of the passive layer increased and that the steady state was not yet reached. Visual observation indicated that no general or pitting corrosion were present on the surface of the 304L, AL-6XN, or 254-SMO samples. XPS analysis (not shown) of the 254-SMO sample showed that the oxide layer is thin and protective, since iron metal can still be observed under the oxide layer and that molybdenum is found in both the V and VI oxidation states.

4.2. Alloys in a 3.55% NaCl in 0.1N HCl solution (0.1N)

In the 0.1N solution, the OCP for 254-SMO and AL-6XN is higher than that of 304L by 100 mV or more (Figure 1(b)). Similar to the Neutral condition, all the alloys in 0.1N solution had an increase in the OCP during the first 72 (or more) hours. However, after that, the OCPs ceased to rise. Based on the OCP alone, the alloys do not become nobler continually in 0.1N as they did in the Neutral. Figures 2(d) and (e) show that in 0.1 N, the corrosion resistance initially increases for the 254-SMO and AL-6XN samples while 304L increases initially followed by a dramatic decrease. This can be clearly observed by the

change in R_p (Figure 3(b)). The R_p values for 254-SMO and AL-6XN rose initially and then seemingly stabilized, while R_p for 304L increased initially, but then decreased considerably. *1/C* plots (Figure 4(b)) show an initial increase in the passive film thickness of alloys 254-SMO and AL-6XN, which is followed by a somewhat stable stage. The values for *1/C* for 304L increase in the beginning and then quickly become erratic, which is indicative of a disintegration of the passive film. This is consistent with the observation, upon completion of the electrochemical studies, that the surface of 254-SMO and AL-6XN did not visually show signs of corrosion, yet pitting corrosion and/or crevice corrosion was clearly visible on the surface of the 304L SS. The Auger results for 304L under the 0.1N condition (not shown) revealed that the exposed area has a much thicker oxide layer than the unexposed area, although the visual observation indicated no difference in the surface condition. This is consistent with the EIS observation that the passive film grew at an early stage, before the pitting process took over causing the film to deteriorate.

4.3. Alloys in a 3.55% NaCl in 1.0N HCl solution (1N)

The OCP for 304L in the 1.0N solution compared with 254-SMO and AL-6XN is much lower (~250 mV) indicating that 304L is considerably less noble than the other two alloys (Figure 1(c)). Both the 254-SMO and AL-6XN showed an initial rise in the OCP after the first few days of exposure. However, toward the end of the study, the OCP began to decrease. Figure 2(g) and 2(h) show an initial rise in corrosion resistance followed by a fall for 254-SMO and AL-6XN. Figure 2(i) shows that the behavior of 304L SS is significantly different from the other alloys, since its corrosion resistance begins to decrease at the initial immersion time. Alloy 254-SMO shows the highest polarization resistance among all three alloys (Figure 3(c)). Both 254-SMO and AL-6XN show a polarization resistance that is approximately three orders of magnitude higher than 304L SS. Inverse capacitance values for alloys 254-SMO and AL-6XN (Figure 4(c)) show that the passive films grow initially, then stabilize, and deteriorate toward the end of the study. For 304L SS, the passive film deteriorated immediately after the test started. The values for 254-SMO were more erratic than AL-6XN, probably due to the instability of the film. Visual inspection after the electrochemical studies showed that the 304L SS had uniform corrosion on the surface, while 254-SMO and AL-6XN appeared corrosion free. This was also observed by SEM (Figure 5).

4.4. Trends in Corrosion Behavior

Values shown on Table 2 indicate that the corrosion rate increased for all the alloys as the acid concentration of the salt solution increased. The increase in corrosion rate based on R_p was most significant for 304L SS, since the final value for passive film resistance decreased by five orders of magnitude. At the conclusion of the study, the alloys 254-SMO and AL-6XN demonstrated to have lower corrosion rates based on values for R_p when compared to 304L SS. Based on R_p values, 254-SMO had the lowest corrosion rate of the three alloys in all acidic conditions at the end of the study. The changes in the R_p values with immersion time were consistent with our previous results of linear polarization tests [10].

The increase in acid concentration decreased the time needed to achieve a steady state. Interestingly, the overall thickness of the passive film (as indicated by *1/C*) on AL-6XN and 254-SMO did not vary considerably. Table 3 shows that the thickness of the passive film, as indicated by the magnitude of *1/C*, decreased with increasing acid concentration, possibly due to an increase in solubility of the passive film in more acidic conditions. However the resistance of the passive film decreased more dramatically. For 254-SMO and AL-6XN, the resistance decreased by three orders of magnitude. It is possible that, with time, the electrolyte is able to infiltrate the passive film decreasing its resistance, but does not influence the capacitance of the film or thickness as dramatically. The passive film formed on 254-SMO seems to allow less penetration by corrosive elements since its R_p values are the

highest. The higher alloyed AL-6XN and 254-SMO performed well under all test conditions, showing little signs of corrosion. This behavior was consistent with their superior performance in the atmospheric exposure study.

There is a clear difference between the performance of 304L and that of AL-6XN and 254-SMO. This can be attributed to the composition of the alloy. 254-SMO and AL-6XN have significantly more Mo and Ni when compared to 304L SS (Table 1). Both Mo and Ni are known for their beneficial effect on corrosion resistance in stainless steel.

Numerous mechanisms on the effects of Mo have been proposed, and they fall into one of the two categories: (1) prevents pit initiation through incorporation into the passive film [11, 12], or (2) facilitates repassivation by reducing active dissolution rate [11-15].

Preventing pit initiation was suggested to be achieved by improving the bonds of the oxide film [16], eliminating pitting nucleation sites [17, 18], or by reversing the ion selectivity [19-21]. All these mechanisms require Mo to be present in the passive film, which is still under debate [22-25]. The results of the surface analysis for 304L support that Mo is enriched in the corrosion product, not in the passive film, yet some Mo in the passive film in high Mo-containing alloys, like AL-6XN were observed.

Reducing the active dissolution rate in a pit can be achieved by the formation of a dissolution barrier inside the pit, in the possible forms of: a salt film layer [26, 27], chlorides and chloride-containing complexes [28], or insoluble molybdates [29, 30]. Although the details are not clearly understood, all mechanisms seem to agree that certain molybdenum containing compound(s) helps to reduce active dissolution of base metal and further facilitates repassivation of stainless steel. The authors think that the beneficial effect of Mo is possibly due to a simpler yet reasonable explanation: Mo chloride ($MoCl_3$) is not soluble in cold water or in dilute acid (including HCl) [31], thus it precipitates on the bottom of the pit, forming a diffusion barrier to prevent further pit growth.

Few reports are available on the mechanisms involving Ni for corrosion resistance of stainless steel. The beneficial effect of Ni is generally recognized in its ability to stabilize the austenitic phase [32]. For instance, it increases the solubility of Mo in the matrix, which in turn enhances the pitting resistance of the steel alloy [33].

Since Ni is nobler than Fe, its presence in stainless steels should improve the corrosion resistance [34]. It has also been found that the addition of Ni to ferritic steel was effective in decreasing the de-passivation pH and the dissolution rate in acidic chloride solutions at crevices [35]. Nishimura proposed that Ni enhances the corrosion resistance of weathering steel in coastal areas through an "iron substitution" mechanism [36], namely, by creating a spinel double oxide, such as Fe_2NiO_4 in an inner rust layer. Kimura confirmed this study, by showing that Ni(II) atoms substitute the Fe(III)-sites of Fe_3O_4 to form $Fe_{3-x}Ni_xO_4$ at the inner layer of the rust, which is negatively charged, and the rust "breathes out" chloride ions from the rust/steel interface [37]. Our surface study showed that a Ni enriched layer formed beneath the surface of the Cr-rich passive film for both 254-SMO and AL-6XN. The location of Ni beneath the Cr-enriched region supports the "iron substitution mechanism" mentioned above; further study on the chemical structure of Ni-containing chemical species is needed to confirm this mechanism.

5. Conclusions

The electrochemical results showed that 254-SMO and AL-6XN have a superior corrosion performance under all test conditions when compared to 304L. Alloy 254-SMO performed slightly better than AL-6XN. The difference in the corrosion resistance of the alloys became more evident as the pH of the 3.55% NaCl solutions decreased.

Under neutral conditions, all three alloys performed well. The values of OCP, R_p and $1/C$ all increased, indicating that the passive films were intact and growing.

Upon completion of the EIS tests in 0.1N HCl salt solutions, the 304L showed clear signs of crevice and pitting corrosion, while 254-SMO and AL-6XN visually remained unchanged. The OCP and R_p values for 304L under 0.1N were lower when compared to Neutral conditions. The value of R_p decreased dramatically after a short period of an initial increase, and the values of *1/C* were erratic during the test. Both observations indicate that the passive film deteriorated. The OCP and R_p values of 254-SMO and AL-6XN were also lower, when compared to those under Neutral conditions, but were much higher than those for 304L. They stabilized after the initial increase, indicating that the passive film was stable and still protective.

Upon completion of the EIS measurements in 1N HCl salt solutions, the 304L underwent general corrosion, and 254-SMO and Al-6XN remained visually unchanged. The OCP, R_p, and *1/C* values for 304L were very low from the beginning, indicating immediate active corrosion from the start of the test. The OCP and R_p values of 254-SMO and AL-6XN were lower in comparison to those obtained under 0.1N conditions. Their values increased slightly initially, then stabilized, and began to slightly decrease toward the end of the test. The *1/C* values were more unstable compared with those obtained under 0.1N conditions, indicating that the passive film starts to experience deterioration but not to the extent that it was visually observable.

The R_p values obtained from the equivalent circuit simulation at the early immersion times were consistent with those obtained by dc electrochemical measurements and were in agreement with the long-term corrosion performance of the alloys as determined in the atmospheric exposure study.

The one year exposure in the natural marine environment at the KSC outdoor exposure facility near the launch pads is more aggressive to 304L SS than immersion for up to 408 hours in the neutral 3.55% NaCl electrolyte solution.

It was concluded that 254-SMO and AL-6XN are suitable alloys to replace the 304L SS currently used at the launch pads and that 254-SMO is expected to perform better than AL-6XN.

Acknowledgements

The authors gratefully acknowledge the funding of this project by the Kennedy Space Center's Director Discretionary Fund (CDDF). The authors also wish to thank Ms. Nancy Zeitlin for her support with project management.

References

1. L. M. Calle and L. G. MacDowell, "Application of Electrochemical Impedance Measurements to Corrosion Prediction in the Space Transportation System Launch Environment", *Corrosion/94*, Paper No. 320, The NACE Annual Conference and Corrosion Show, Houston, TX: NACE, 1994.
2. L. M. Calle and L. G. MacDowell, "Electrochemical Impedance Spectroscopy of Metal Alloys", *NASA Tech Briefs* journal, Volume 17, p 66, January 1993.
3. C. Ontiveros and L. G. MacDowell, Corrosion 90, Paper No. 94, NACE (1990)
4. L. M. Calle and L.G. MacDowell, "Study of Metal Corrosion Using AC Impedance Techniques in the Space Transportation System (Space Shuttle) Launch Environment," *ADVMAT/91, First International Symposium on Environmental Effects on Advanced Materials*, Houston, TX: NACE, 1991.
5. R.G. Barile, L.G. MacDowell, J. Curran, L.M. Calle, and T. Hodge, "Corrosion of Stainless Steel Tubing in a Spacecraft Launch Environment," Corrosion/2002, Paper No. 02152, The NACE Annual Conference and Corrosion Show, Houston, TX: NACE, 2002.

6. D.C. Silverman, Primer on the AC Impendence Technique", in: Electrochemical Techniques for Corrosion Engineering, Ed. R. Baboian, NACE (1987) p73
7. K.M. Ismail, S.S. El-Egamy, and M. Abdelfatah, *Journal of Applied Electrochemistry* **31** (2001) 663.
8. K. M. Ismail, A. M. Fathi, and W. A. Badawy, *Corrosion* **60** (2004) 795.
9. H.H. Huang, W.T. Tsai, and J.T. Lee, *Electrochimica Acta* **41** (1996) 1191.
10. L.M. Calle, R.D. Vinje, and L.G. MacDowell, "Electrochemical Evaluation of Stainless Steels in Acidified Sodium Chloride Solutions," CORROSION/2004, Paper No. 04303 (Houston, TX: NACE 2004).
11. K. Sugimoto and Y. Sawada, *Corrosion Science* **17** (1977) 425.
12. Ya.M. Kolotyrkin, and L.I. Freiman, in: Korroziya i Zashchita ot Korroziy, vol. 5, Izd. WINITI, Moscow, 1978, p. 5.
13. H. Ogawa, H. Omata, I. Itoh, and H. Okada, *Corrosion* **34** (1978) 53.
14. R.C. Newman, *Corrosion Science.* **25** (1985) 331.
15. H.C. Brookes, F.J. Bayles, and F. J. Graham, *Journal of Applied Electrochemistry* **20** (1995) 223.
16. W.R. Cieslak, and D.J. Duquette, *Journal of The Electrochemical Society* **132**, (1985) 533.
17. V. Mitrovic-Scepanovic, and M.B. Ives, *Journal of The Electrochemical Society* **127** (1985) 1903.
18. P. Marcus and M. Moscatelli, *Journal of The Electrochemical Society* **136** (1989) 1634.
19. M. Sakashita and N. Sato, *Corrosion* **35** (1979) 351.
20. Y.C. Lu, C.R. Clayton, and A.R. Brookes, *Corrosion Science* **29** (1989) 863.
21. M. Sakashita, and N. Sato, In Frenkental, Kruger (Eds.) Passivity of Metals. The Electrochem. Soc., Pennington, 1978, p. 479
22. G. O. Ilevbare and G. T. Burstein, *Corrosion Science* **43** (2001) 485.
23. J. R. Galvele, J. B. Lumsden, and R. W. Staehle, *Journal of The Electrochemical Society* **125** (1978) 1204.
24. C.G. Barnes, A.W. Aldag, and R.C. Jerner, *Journal of The Electrochemical Society* **119** (1972) 684.
25. R. Goetz, and D. Landolt, *Electrochimica Acta* **29** (1984) 667.
26. A. Guenbour, J. Faucheu, and A. Ben Bachir, *Corrosion* **44** (1988) 214.
27. A. Schneider, D. Kuron, S. Hofmann, and R. Kirchheim, *Corrosion Science* **31** (1990) 191.
28. I. Olefjord, B. Brox, and U. Jelvestam, *Journal of The Electrochemical Society* **132** (1985) 2854.
29. G. Ruijini and M.B. Ives, *Corrosion* **45** (1989) 572.
30. F.A. Cotton and G. Wilkinson, Advances in Inorganic Chemistry, Wiley, New York, 1988.
31. CRC Handbook of Chemistry and Physics, 73rd, Ed. David R. Lide, CRC Press, Boca Raton, Florida (2000)
32. A.A. Hermas, K. Ogura, S.Tagaki, and T. Adachi, *Corrosion* **51** (1995) 3.
33. Yu. I. Bil'chugov, N.L. Makarova, and A.A. Nazarov, *Protection of Metals* **37** (2001) 597.
34. J.H. Qiu, *Surface and Interface Analysis* **33** (2002) 830.
35. S. Azuma, T. Kudo, H. Miyuki, M. Yamashita, and H. Uchida, *Corrosion Science* **46** (2004) 2265.
36. Toshiyasu Nishimura and Toshiaki Kodama, *Corrosion Science* **45** (2003) 1073.

37. M. Kimura, H. Kihira, M. Nomura, and Y. Kitajima, Corrosion protection mechanism of the advanced weathering steel (Fe-3.0Ni-0.40Cu) in a coastal area, Meeting of The Electrochemical Society, Honolulu, Hawaii, October 3-8, 2004.